Combining multideterminantal wave functions with density functionals to handle near-degeneracy in atoms and molecules

R. Pollet and A. Savin
Laboratoire de Chimie Théorique, CNRS et Université Pierre et Marie Curie, Paris, France

T. Leininger
Laboratoire de Physique Quantique, CNRS et Université Paul Sabatier, Toulouse, France

H. Stoll
Institut für Theoretische Chemie, Universität Stuttgart, Stuttgart, Germany

(Received 6 March 2001; accepted 6 November 2001)

Control of near-degeneracy effects and dynamical correlation in atoms and molecules is within sight, thanks to an economical method that mixes configuration interaction (CI) and density functional theory (DFT). The influence of the size of the configuration-space has been studied for light systems including elements of the first and second period of the Periodic Table. © *2002 American Institute of Physics.* [DOI: 10.1063/1.1430739]

I. INTRODUCTION

Different approaches are usually available for the quantum chemist in order to deal with dynamical (interelectronic repulsions at short-range) or nondynamical (near-degeneracy or rearrangement of electrons within partially filled shells) correlation.[1] The analysis of the Fermi and Coulomb holes (see, e.g., Ref. 2) can be helpful in picturing both components and in grasping the nature of their physical origins.

Because of ''left–right'' correlation, it is commonly believed that the exchange-correlation hole in a molecule is localized around the reference electron (see, e.g., Ref. 3). In fact, this is especially true at large internuclear distance, where the total hole is localized around the nearest nucleus to the reference electron, whereas at smaller distance there still exists a weak contribution to the hole on the other nuclei. By comparison, the hole of the homogeneous electron gas always strictly ''follows'' the reference electron. The Kohn–Sham method (KS) (Ref. 4) can give rise to such localized model holes, with the help of approximate exchange-correlation functionals such as LSDA (Ref. 4) or GGA (see, e.g., Refs. 5–8), which depend on the density or the gradient of the density. While the approximate correlation functionals efficiently model dynamical correlation, local exchange functionals can also mimic part of the nondynamical correlation, in addition to the exchange energy (see, e.g., Ref. 9). It results in a crude description of nondynamical correlation.

A much-discussed problem is that of symmetry-breaking, where the ability to cover these near-degeneracy effects has serious consequences (see, e.g., Ref. 10). For example, hybrid functionals can strongly increase the tendency to break spatial symmetry as soon as one augments the weight of the Hartree–Fock delocalized exchange. The resulting poor quality of the atomic or molecular wave function then restricts its use in applied theoretical chemistry (i.e., calculations of vibrational frequencies, study of bond-breaking reactions, determination of reaction barriers of transition states, ...).

Other alternatives that aim to describe this nondynamical correlation, inside the DFT formalism, are ensemble theory[11] and the fractional occupation number (FON) method.[12–15] The former approach asserts that, for systems with a strong multideterminantal character, the interacting density can only be represented by an ensemble of degenerate monodeterminantal states. The latter is based on Janak's theorem,[16] which allows fractional occupations on frontier orbitals, hence a simulation of a mixing of configurations.

More traditionally, quantum chemists often use the wave function formalism, and especially configuration interaction (CI), to deal with nondynamical correlation. The inherent process is then to compensate the long-range delocalized exchange hole of the reference wave function by building a long-range correlation hole.[3]

Consequently, it seems natural to try to combine CI with DFT (for a review, see Ref. 17), with the secret hope to get the better of both worlds (i.e., low ''CPU cost/accuracy'' ratio and ease of interpretation for DFT, explicit handling of near-degeneracies and possibility of systematic improvement for CI), to deal with systems where dynamical as well as nondynamical correlation are crucial. Adding a localized correlation hole, by a DFT contribution, to a correlation hole that already compensates the exchange hole at long range, should yield an exchange-correlation hole that is somewhat localized around the reference electron. The combination can be achieved by splitting the two-electron operator, with one part dedicated to CI and the other to DFT. The proportion of each component can then be adjusted by varying a coupling parameter.

After a brief recall of the underlying theory and a survey of technical details, we will explore a few systems and stress the importance of the choice of the coupling parameter. Depending on the inherent multideterminantal character of the atom or molecule, only a small or medium configuration-space will be necessary, resulting in an inexpensive computation.

II. THEORY

Straightforward mixing of CI and DFT techniques can result in a double counting of correlation contributions. To prevent this artifact, the key technique is to split the interacting Hamiltonian.[18–21] This separation can be made with the help of the standard error function,

$$\hat{V}_{ee}=\hat{V}_{\mathrm{sr}}+\hat{V}_{\mathrm{lr}}, \tag{1}$$

$$\hat{V}_{\mathrm{lr}}=\frac{1}{2}\sum_{i\neq j}^{N} v_{\mathrm{lr}}(\mathbf{r_i},\mathbf{r_j}), \tag{2}$$

$$v_{\mathrm{lr}}(\mathbf{r_i},\mathbf{r_j})=\frac{\mathrm{erf}(\mu|\mathbf{r_i}-\mathbf{r_j}|)}{|\mathbf{r_i}-\mathbf{r_j}|}, \tag{3}$$

where $\hat{V}_{\mathrm{sr}}$ and $\hat{V}_{\mathrm{lr}}$ are, respectively, the short- and long-range two-electron operators. These two-electron operators are chosen so that the short-range one presents a singularity at electron–electron coalescence, while the smooth long-range one possesses the Coulomb tail. The calculation of bielectronic integrals is also more convenient with operators involving the error function than with other operators that were chosen in the past, like the Yukawa two-electron operator.[20] As a starting point, the coupling parameter μ is chosen to be position-independent.

The short-range part of the interelectronic operator will be handled by density functionals, while the long-range part will be described by a multideterminantal wave function. Thus, since

$$\begin{cases} \mathrm{erf}(0)=0 \\ \mathrm{erf}(+\infty)=1, \end{cases}$$

the pure Kohn–Sham method can be fully recovered at $\mu=0$, while a complete CI occurs as $\mu\rightarrow+\infty$.

The ground state electronic energy E_0 can be obtained by the constrained-search formalism[22] below,

$$E_0=\min_{\rho} E_v[\rho] \tag{4}$$

$$=\min_{\rho}\left\{F[\rho]+\int v(\mathbf{r})\rho(\mathbf{r})d\mathbf{r}\right\} \tag{5}$$

$$=\min_{\Psi}\left\{\langle\Psi|\hat{T}+\hat{V}_{\mathrm{lr}}|\Psi\rangle+U_{\mathrm{sr}}[\rho(\Psi)]+E_{\mathrm{xc,sr}}[\rho(\Psi)]+\int v(\mathbf{r})\rho(\mathbf{r})d\mathbf{r}\right\}, \tag{6}$$

where v is the external potential, $\rho=\rho(\Psi)$ is the interacting density corresponding to the multiconfigurational wave function Ψ, F is the universal density functional, $\hat{T}$ is the kinetic energy operator, U_{sr} is the short-range Hartree energy, and $E_{\mathrm{xc,sr}}$ is the short-range exchange-correlation energy.

Because the long-range two-electron operator shows no singularity at electron–electron coalescence, this partitioning has the advantage to release the CI calculation, in a finite set of one-particle basis functions, from trying to represent the cusp. Thus, a smaller configuration-space should be sufficient for an accurate calculation.

For the DFT part, the spin-independent local density approximation (LDA) was used. That reinforces the chosen split of the electron–electron interaction, as leaving DFT cover the short-range domain will enable the transferability of short-range correlation effects (supposed to be independent of the system) from the homogeneous electron gas. We expect that our results should not suffer too much from not using density gradient corrections for the short-range correlation energies, as noted by Perdew *et al.*[23] Whereas the short-range local exchange functional can be obtained analytically, a local correlation functional has to be designed for the short-range interaction. This has been achieved by interpolating some coupled-cluster (CC) calculations, made by following Freeman,[24] on the homogeneous electron gas for various μ and r_s (Wigner–Seitz radius). This led to premultiply the VWN correlation energy functional[25] by a short-range correction factor.[26] One has, nevertheless, to qualify the physical meaning of this correction. These coupled-cluster calculations yielded long-range correlation energy densities, from which we deduced short-range ones by subtracting them from Coulomb results. Thus, the ''short-range'' correction actually also contains coupling terms between long- and short-range contributions.

If we want to predict the approximate value of the coupling parameter that will yield the most accurate result for a given system, we can rely on the specific case of the spin-unpolarized homogeneous electron gas. In that case, μ must depend on the electronic density, in an unknown way. We can try a simple local approximation $\mu(\rho)$ on the basis of the fact that an electron occupies on average the sphere delimited by the Wigner–Seitz radius $r_s=[3/(4\pi\rho)]^{1/3}$. If we model the short-range correlation as becoming significant when one electron penetrates the occupation sphere of the other, we can try

$$\mu(\rho)=\frac{1}{r_s} \tag{7}$$

as a starting point.

The expression of the resulting short-range exchange energy per electron, which is the analog of the total one, is

$$\epsilon_{x,\mathrm{sr}}=\int_0^{\infty} 2\pi u\ \mathrm{erfc}(\mu(\rho)u)\rho_x(u), \tag{8}$$

where $u=|\mathbf{r_1}-\mathbf{r_2}|$ and $\rho_x(u)$ is the density of the Fermi hole.[27] We can picture how this hole is modified by the short-range electron–electron interaction, by considering the function,

$$f(u)=\mathrm{erfc}(\mu(\rho)u)\rho_x(u). \tag{9}$$

Figure 1 shows a comparison of these two functions for $r_s=2$.

We can see that applying the short-range interaction sharpens the Fermi hole at short interelectronic distance, while the oscillations at long-range nearly vanish (not shown on the figure).

Now we consider the resulting short-range correlation energy. Within the local approximation (7), we succeeded in fitting the short-range correction factor to the VWN correlation functional in the case of the unpolarized homogeneous

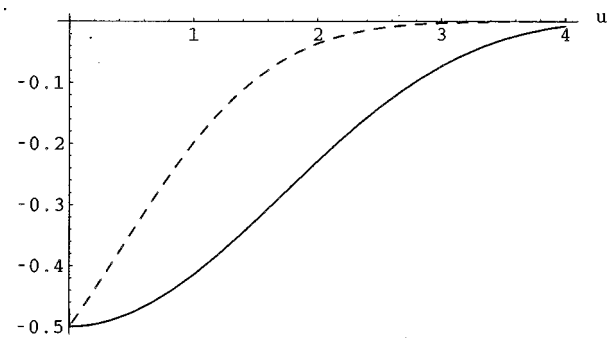

FIG. 1. Fermi hole, $\rho_x(u)$, divided by the density ρ, in the spin-unpolarized homogeneous electron gas for $r_s=2$ (solid line) and the function obtained by multiplication of the complementary error function erfc $[\mu(\rho)u]$ (dashed line). u is the interelectronic separation in bohrs.

electron gas. Its expression is $\alpha r_s^\beta/(1+\alpha r_s^\beta)$, where $\alpha=0.816\,28$ and $\beta=0.242\,74$. We have tested the validity of this approximate short-range correlation energy when applied to atoms and molecules. In Fig. 2, the correlation energies of 54 systems including atoms, ions, hydrides, dimers, and the isoelectronic series of helium and beryllium,[28] are compared with experience.

Although a non-self-consistent numerical program was used, we can observe that, overall, the well-known overestimation tendency of the LSDA correlation energy (by a factor of roughly 2) is corrected by only retaining the short-range contribution. This success is all the more striking since no spin polarization correction was used for the short-range correlation functional, neither within the framework of conventional spin density functional theory nor within its alternative interpretation in terms of the on-top pair-density.[29–32]

Typical examples that fail to be described by a short-range correlation functional are the HF hydride, and the C_2, N_2, O_2, and F_2 dimers. Lie and Clementi[33,34] found that 2, 4, 10, 5, and 2 CSF's were respectively needed in order to obtain a proper dissociation of these molecules. Thus, we expect that the combination of short-range density functionals with CI will correct these results by taking into account the nondynamical correlation.

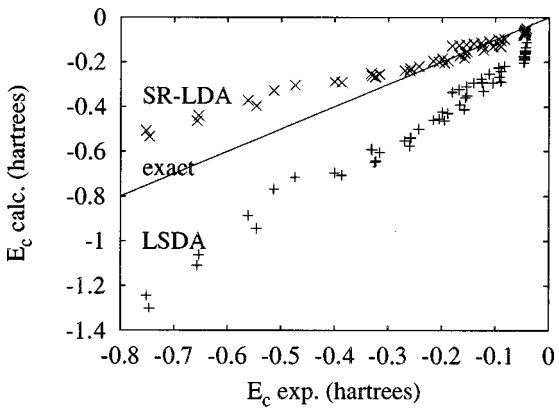

FIG. 2. Comparison of LSDA and short-range LDA correlation energies with experimental data for a set of 54 atomic and molecular systems (Ref. 28).

In order to perform the CI-DF coupling, it is easier to use a position-independent coupling parameter. Thus, a convenient way to transfer what we have learned from the spin-unpolarized homogeneous electron gas to atoms and molecules is to introduce a system-averaged coupling parameter,

$$\langle\mu\rangle=\frac{1}{N}\int\mu[\rho(\mathbf{r})]\rho(\mathbf{r})d\mathbf{r}. \tag{10}$$

For the local approximation (7),

$$\langle\mu\rangle=\langle r_s^{-1}\rangle \tag{11}$$

$$=\left(\frac{4\pi}{3}\right)^{1/3}\int\rho^{4/3}(\mathbf{r})d\mathbf{r}, \tag{12}$$

which is easily computed because it is proportional to Dirac's local exchange.[35] In spite of this crude system-average (it can only give a "compromise" value between several regions), interesting results will be presented in the next sections. Beside this system-averaged coupling parameter, we also expect that there exists an intermediate value of μ, between 0 (KS) and ∞ (CI), that will yield the closest energy to the exact one. Searching for such a value will however lead to a violation of size extensivity and size-consistency. The problem could occur for example when heteronuclear molecules dissociate. As the optimal μ's of the fragments may be quite different, the sum of the corresponding energies may not be equal to the energy of the molecule at infinite separation at its own optimal μ.

III. TECHNICAL DETAILS

Our primary goal was to find the smallest configuration-space that ensures a good accuracy, in order to enlarge the scope of applications of the CI class of methods, that are still computationally demanding. The study of a systematic improvement that consists in including more and more configuration state functions (CSF) in the CI expansion implies to sort the orbitals in order of importance. In all the calculations presented below, we decided not to optimize the orbitals, which should be done in practical applications of the method by coupling density functionals with MCSCF wave functions, but to use accurate natural spin–orbitals[36] to build the CSF's. They are the eigenfunctions of the reduced first-order density operator $\hat{\gamma}_1=\Sigma_i n_i|\phi_i\rangle\langle\phi_i|$, where the occupation number n_i obeys the Pauli condition $0\leqslant n_i\leqslant 1$. We justify this preference mainly because mixing the natural orbitals provides an accurate description of the nondynamical correlation. Moreover, the observation of their occupation number reveals their probable importance in the CI (a large occupation number indicates weightiness, whereas a small one can lead to omit the natural orbital without dramatically penalize the efficiency of the expansion). Prior to the coupling, a MRCI calculation will therefore be necessary to produce reliable natural orbitals. This has been achieved by choosing a cutoff value for the occupation numbers equal to 0.01 for all the systems.[37] Please note that this required calculation is on no account a part of the CI-DF coupling but that we need it for our study of a systematic improvement. We will also make use of this calculation to obtain the reference correlation energy, in the case of BeH, BH, B_2, and O_2. For He and

H_2, however, "exact" results will be used, while for Be, H_2 at large internuclear distance, LiH, and Li_2, full CI results will be used. All these results can be found in the captions of the tables that appear in the Results and Discussion.

Large uncontracted basis sets have been used for each atom of the systems studied below. These are Dunning's correlation-consistent polarized valence basis sets,[38,39] i.e., cc-pV5Z $(8s4p3d2f)$ for H and He, cc-pVQZ $(12s6p3d2f)$ for Li, cc-pV5Z $(14s8p4d3f)$ for Be, B, Ne, and O. The Stuttgart pseudopotentials[40] have helped to reduce the CPU time and to focus on effects specific to the valence shell. Calculations on diatomics use experimental equilibrium bond distances (cf. Table VI in Refs. 33 and 34). The radial part of the DFT integration grid is based on the transformation $r=-\alpha \log_e(1-x^{m_r})$,[41] while the angular part is a Lebedev quadrature scheme.[42]

The whole scheme was incorporated in the Molpro package of *ab initio* programs,[43] in the multireference configuration interaction (MRCI) code.[44,45] Care has also been taken to the modification of the bielectronic integrals, to suit the long-range operator.[46] During the calculation, upgrading the density matrix enables the CI coefficients optimization, while the orbitals remain frozen. This explains why the CI-DF energy of a single determinant at $\mu=0$ is not the "true" Kohn–Sham energy, and why as $\mu\to\infty$ the energy is above the Hartree–Fock one. Nevertheless, we will still use Kohn–Sham and Hartree–Fock terms to describe CI-DF at $\mu=0$ and $\mu\to\infty$.

IV. RESULTS AND DISCUSSION

The purpose of this section is to pass in review many-electrons systems that will exhibit a growing multideterminantal character. This means that a calculation on the first systems ("normal" systems) presented will reach a good accuracy (more than 75% of the correlation energy) with only one Slater determinant, while the last systems ("abnormal" systems) will truly need additional configurations to describe their ground state in an accurate way. Typically, we will focus on the variation of the electronic energy or the correlation energy, defined as the difference between the energy and the restricted Hartree–Fock (RHF) energy, with μ for larger and larger configuration spaces. The first point to note will be the smallest value of the coupling parameter that will yield the most accurate result to within about 0.05% (such a value will be called from now on the "best" μ). Then, we will have to determine which is the smallest configuration-space, around that value, that preserves a reasonable accuracy.

A. "Normal" systems

1. Helium atom

The helium atom is a good illustration of a system where near-degeneracy correlation effects are not significant. It is shown in Fig. 3, where we have plotted the variation of energy with the coupling parameter for two configuration spaces. It appears that the monodeterminantal wave function reaches a good accuracy if we focus on a domain surrounding $\langle\mu\rangle=0.96\,\mathrm{bohr}^{-1}$ (which was computed from the RHF electron density[47]).

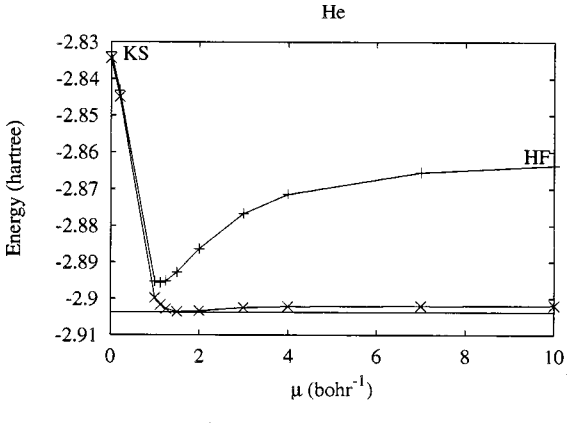

FIG. 3. Variation of the energy of helium with the CI-DF coupling parameter: the upper curve represents the calculation using the configuration $(1s)^2$ only, the lower curve was obtained by adding the natural orbitals $2s$, $2p$, $3s$, $3p$, $3d$ to the configuration space, and the horizontal line is the exact energy (Ref. 48).

In fact, the value of the coupling parameter that yields the closest energy to the "exact" one occurs at 1.125 bohr^{-1} for the $(1s)^2$ configuration. Here, the percentage of error on the energy is less than 0.3%. Moreover, the electronic energy is lowered by almost 63 millihartree compared to standard Kohn–Sham $(\mu=0)$, and almost 34 millihartree compared to Hartree–Fock $(\mu\to\infty)$. This important improvement emphasizes the quality of the short-range local density approximation in comparison to the conventional one. Furthermore, our short-range approximate density functional is spin-unpolarized, and yet yields rather accurate results.

In short, we can greatly reduce the computational cost by limiting the CI to only one CSF if we choose μ around 1 bohr^{-1}. Obviously, if we enlarge the configuration-space by including up to $3d$ natural orbitals, the error can reach only 0.004% at the "best" μ (around 1.5 bohr^{-1}). It is worth mentioning that this is in better agreement with the exact energy than the pure CI result.

The details of the systematic calculations are revealed in Table I, where we have listed each natural orbital, its occupation number, the corresponding number of CSF's, and the percentages of correlation energy at "best" μ, system-averaged μ, and for pure CI. Here again, we can see that a very good accuracy appears much earlier for an appropriate CI-DF coupling than for a traditional CI. In fact, the CI-DF coupling is much superior to the CI until the $2p$ NO is incorporated to the configuration-space. Therefore, although the large occupation number of the $1s$ NO seems to minimize importance of the other NO's, the $2p$ NO makes a significant contribution to the correlation energy, which is called "angular correlation," just as well in the traditional CI as, to a certain extent, in the CI-DF coupling. After the inclusion of the $3p$ NO, the results given by the system-averaged μ deteriorate while the "best" μ will still perform better than the CI.

In order to emphasize the role of the DFT component in

TABLE I. He: Changes of the correlation energy with increasing configuration space. From one line to the next, it changes by the addition of the natural orbital (NO). Its occupation number (ON), in the MRCI reference calculation is also given, as is the total number of configuration state functions (CSF). The correlation energy obtained with the smallest ("best") coupling parameter μ yielding an error lower than 0.05%, that with the system-averaged coupling parameter $\langle r_s^{-1}\rangle$, and that obtained in a pure configuration interaction calculation ($\mu\to\infty$), for the corresponding space, are given as a percentage of the "exact" correlation energy, defined as the difference between the exact and Hartree–Fock energies. $E_{\text{exact}}=-2.9037$ a.u. (Ref. 48), $E_{\text{RHF}}=-2.8616$ a.u., $\langle r_s^{-1}\rangle=0.96$ bohr^{-1}.

			Percentage of correlation energy		
NO	ON	CSF's	"best" μ	$\langle r_s^{-1}\rangle$	$\mu\to\infty$
$1s$	1.983 920 1	1	79.9	79.0	−0.1
$2s$	0.007 596 5	3	83.8	80.7	38.5
$2p$	0.002 559 8	6	97.1	86.7	85.0
$3s$	0.000 125 2	9	97.8	87.4	87.0
$3p$	0.000 082 1	15	99.2	88.7	90.9
$3d$	0.000 064 7	27	99.7	88.8	95.1
$4s$	0.000 007 8	33	99.8	88.9	95.3

the energy lowering, we have to check that its contribution is not already very small around 1 bohr^{-1}. Figure 4 contradicts this hypothesis by showing the variation of the short-range exchange-correlation energy for the $(1s)^2$ configuration along the coupling. It reveals that, at 1.125 bohr^{-1}, its contribution to the energy is still large (−290 mhartree), proving the importance of short-range DF effects in order to properly describe dynamical correlation.

2. Hydrogen molecule

In H_2 at the equilibrium bond distance, the absence of nondynamical correlation effects is even more pronounced than in helium. This is shown in Table II, where 84% of the correlation energy is recovered with a single Slater determinant, in spite of a smaller occupation number of the first NO than in helium.

Here, the $1\sigma_u$ and $1\pi_u$ NO's play a role comparable to the $2p$ NO in helium, inasmuch as their contribution to the correlation energy is crucial to the efficiency of pure CI and important for the CI-DF coupling.

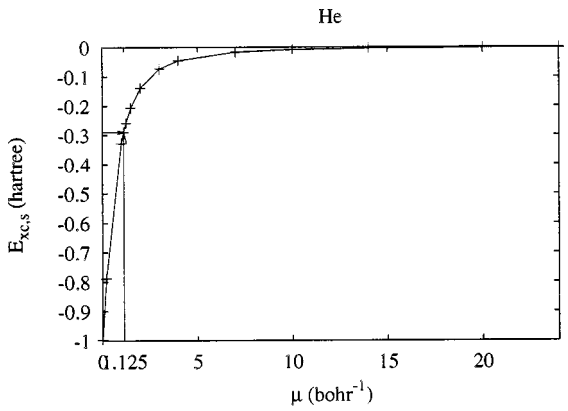

FIG. 4. Variation of the short-range exchange-correlation energy with the coupling parameter for the $(1s)^2$ configuration of helium.

TABLE II. H_2: Changes of the correlation energy with increasing configuration space. For the explanation of symbols, see Table I. $E_{\text{Exact}}=-1.1735$ a.u. (Ref. 49), $E_{\text{RHF}}=-1.1336$ a.u., $\langle r_s^{-1}\rangle=0.62$ bohr^{-1}.

			Percentage of correlation energy		
NO	ON	CSF's	"best" μ	$\langle r_s^{-1}\rangle$	$\mu\to\infty$
$1\sigma_g$	1.964 258 2	1	84.0	84.0	−0.3
$1\sigma_u$	0.019 870 1	2	88.7	88.6	46.3
$2\sigma_g$	0.006 025 7	4	90.4	89.5	64.9
$1\pi_u$	0.004 267 6	6	97.2	92.8	91.2
$3\sigma_g$	0.000 199 4	9	97.4	92.8	92.5
$2\sigma_u$	0.000 191 5	11	98.2	93.6	93.7
$1\pi_g$	0.000 144 3	13	98.6	93.6	95.6

3. LiH hydride

In LiH, correlation effects are also dominated to a large extent by dynamical correlation. This can be seen in Table III by observing the high percentage of correlation energy that is recovered with only one Slater derminant for the CI-DF coupling. We should mention here that when the totality of the correlation energy is recovered with the largest configuration-space at "best" μ, percentages greater than 100% were also found around that value, emphasizing the fact that the CI-DF method is no longer variational, as soon as one had to choose an approximate short-range exchange-correlation functional. Thus, the energy at $\mu=0.75$, when the 6σ orbital is included, lies below that of the full CI by 0.2%. Note please that this is actually not a proof of the nonvariational character, as our full CI energy is just an upper bound to the exact energy. As a pseudopotential was used for Li, we have no better estimates in the literature.

Here again, and despite a small occupation number, the 1π NO makes a significant contribution both in CI-DF and CI techniques. It is also worth noting the very good performance of the system-averaged coupling parameter, as the percentage of correlation energy stays very close to that at "best" μ (within slightly more than 1%).

4. Li_2 dimer

As can be seen in Table IV, the virtual NO's of the Li_2 dimer have rather large occupation numbers, which could question the efficiency of a monodeterminantal wave function. Nevertheless, the CI-DF coupling still performs accurately even with a single configuration. The contributions to

TABLE III. LiH: Changes of the correlation energy with increasing configuration space. For the explanation of symbols, see Table I. $E_{\text{FCI}}=-0.7870$ a.u., $E_{\text{RHF}}=-0.7501$ a.u., $\langle r_s^{-1}\rangle=0.45$ bohr^{-1}.

			Percentage of correlation energy		
NO	ON	CSF's	"best" μ	$\langle r_s^{-1}\rangle$	$\mu\to\infty$
2σ	1.941 223 1	1	89.0	89.0	−0.4
3σ	0.029 100 3	3	90.9	90.9	43.7
1π	0.010 000 5	5	95.9	95.6	77.4
4σ	0.008 008 5	8	98.4	97.3	91.9
5σ	0.000 304 6	12	99.1	97.9	93.2
2π	0.000 233 4	16	99.8	98.5	95.0
6σ	0.000 132 1	21	100.0	98.9	95.7

TABLE IV. Li_2: Changes of the correlation energy with increasing configuration space. For the explanation of symbols, see Table I. $E_{FCI}=-0.4307$ a.u., $E_{RHF}=-0.3981$ a.u., $\langle r_s^{-1}\rangle=0.22$ bohr^{-1}.

			Percentage of correlation energy		
NO	ON	CSF's	"best" μ	$\langle r_s^{-1}\rangle$	$\mu\to\infty$
$2\sigma_g$	1.811 885 2	1	83.2	83.2	−0.8
$1\pi_u$	0.063 117 0	3	90.5	90.5	68.1
$3\sigma_g$	0.031 432 9	5	92.0	91.1	86.3
$2\sigma_u$	0.029 321 1	6	100.0	94.5	98.3

the correlation energy yielded by the $1\pi_u$ and $2\sigma_u$ are, however, quite significant. Actually, as the $2\sigma_u$ NO is included, the correlation energy recovered by the CI is greater than by the CI-DF coupling with the system-averaged μ, but still lower if we consider the "best" μ.

As in the LiH hydride, the CI-DF coupling yielded more correlation energy for the largest configuration-space around the "best" μ than the full CI did. This effect is even more pronounced than in LiH, as the energy at $\mu=0.75$, when the $2\sigma_u$ orbital is included, lies below that of the full CI by 3.1%.

5. O_2 dimer

O_2 at equilibrium bond distance almost exhibits no nondynamical correlation effects. This can be seen in Table V, as one can retrieve 87.8% of the correlation energy with only one CSF, if the "best" μ is chosen.

One can also note the great advantage to use CI-DFT with "best" μ as well as system-averaged μ over pure CI. Moreover, adding more than one CSF improves only slightly the results.

B. "Abnormal" systems

1. Be series

We now step into systems with a fairly large amount of nondynamical correlation. The beryllium isoelectronic series is a sequence where strong near-degeneracy effects occur in the *L*-shell. As a matter of fact, the large occupation number of the $2p$ NO, reported in Table VI, suggests taking the $(1s)^2(2p)^2$ configuration into account for an accurate calculation.

This also appears in Fig. 5, where three calculations are shown, each corresponding to a different configuration-space. Even if the monodeterminantal wave function, at "best" μ, yields an energy which is, respectively, 9 and 32 millihartree lower than at $\mu=0$ (Kohn–Sham) and $\mu\to\infty$ (Hartree–Fock), still demonstrating the efficiency of the CI-DF coupling, it is now perfectly clear that a single configuration is not enough to represent the ground state of that system. Even at the "best" μ, the monodeterminantal wave function indeed yields an electronic energy with an error greater than 1.6% in comparison to the lowest energy obtained with the largest CI. Whereas, if we consider a larger configuration-space by including the $2p$ natural orbitals, the curve becomes closely parallel to that of the larger CI.

TABLE V. O_2: Changes of the correlation energy with increasing configuration space. For the explanation of symbols, see Table I. $E_{MRCI}=-31.9535$ a.u., $E_{RHF}=-31.4576$ a.u., $\langle r_s^{-1}\rangle=1.08$ bohr^{-1}.

			Percentage of correlation energy		
NO	ON	CSF's	"best" μ	$\langle r_s^{-1}\rangle$	$\mu\to\infty$
$1\pi_g$	1.023 870 9	1	87.8	70.2	−0.6
$1\pi_g$	1.023 870 9	2	88.7	75.2	7.2
$3\sigma_u$	0.051 158 8	48	90.1	81.6	21.2
$2\pi_u$	0.157 44 5	2588	91.8	85.2	31.6
$4\sigma_g$	0.010 355 0	12282	92.6	86.7	36.8
$4\sigma_u$	0.007 331 9	47856	92.9	87.6	41.7

TABLE VI. Be: Changes of the correlation energy with increasing configuration space. For the explanation of symbols, see Table I. $E_{FCI}=-1.0109$ a.u., $E_{RHF}=-0.9628$ a.u., $\langle r_s^{-1}\rangle=0.32$ bohr^{-1}.

			Percentage of correlation energy		
NO	ON	CSF's	"best" μ	$\langle r_s^{-1}\rangle$	$\mu\to\infty$
$2s$	1.810 928 2	1	66.2	63.7	−1.6
$2p$	0.061 842 0	4	96.8	73.2	95.8
$3s$	0.002 797 9	6	99.5	73.9	98.6
$3d$	0.000 106 6	16	100.0	73.9	99.4

Furthermore, one can note the rather poor performance of the CI-DF coupling with the system-averaged coupling parameter, and the possible hidden nonvariational character of the CI-DF method, as the energy at $\mu=2.25$, when the $3d$ orbital is included, lies below that of the full CI by 0.2%.

Now we will try to grasp the nature of the coupling parameter by comparing Be and Ne^{6+}, which belong to the beryllium isoelectronic series. Figure 6 illustrates the increase of near-degeneracy effects with the atomic number

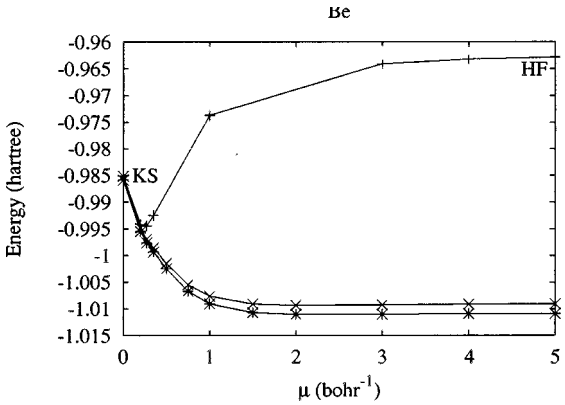

FIG. 5. Variation of the energy of beryllium with the CI-DF coupling parameter: the upper curve represents the calculation using the configuration $(2s)^2$ only, the next curve was obtained by adding the $2p$ natural orbitals to the configuration-space, the lower curve was obtained by adding the natural orbitals $2p$, $3s$, $3d$, $4s$, $3p$ to the configuration space, and the exact energy can be estimated by the value at the end of the lower curve.

TABLE VII. Be: Dependence of the "best" coupling parameter μ on the size of the configuration space (for the definition of the "best" μ, see first paragraph of the Results and Discussion). The corresponding short-range exchange correlation energy contribution is also given. $E_{\mathrm{FCI}} = -1.0109$ a.u., $E_{\mathrm{RHF}} = -0.9628$ a.u.

NO	"best" μ	$E_{\mathrm{sc,sr}}$
$2s$	0.25	-0.165
$2p$	2.00	-0.009
$3s$	2.25	-0.007
$3d$	1.80	-0.007

(the curves have been shifted to show the respective energy lowerings). Here, we will limit the size of the configuration-space to the $(1s)^2(2p)^2$ configuration previously identified as important. As expected, the nondynamical correlation is much greater for the ion ($Z=10$) than for the atom ($Z=4$). Furthermore, a shift can be observed in the "best" μ [around 0.3 bohr^{-1} for Be and 1.5 bohr^{-1} for Ne^{6+}, for the $(1s)^2(2s)^2$ curve]. To understand that feature, one has to remember that the inverse of the coupling parameter $1/\mu$ acts like an effective interaction distance, which decreases when Z increases. This example underlines the importance of using a position-dependent coupling parameter.

2. H_2 dimer at large bond distance

Near-degeneracy correlation often arises in dissociating molecules. For example, whereas nondynamical correlation effects do not prevail in H_2 at the equilibrium bond distance, a completely different situation appears when $R=3.0$ bohr.

This can be seen in Table VIII, where we can relate the small percentage of correlation energy recovered by the single Slater determinant wave function to the large occupation number of the $1\sigma_u$ NO. Also important is the role played by the $1\pi_u$ NO in the improvement of the correlation energy. But, as in the case of the beryllium atom, adding

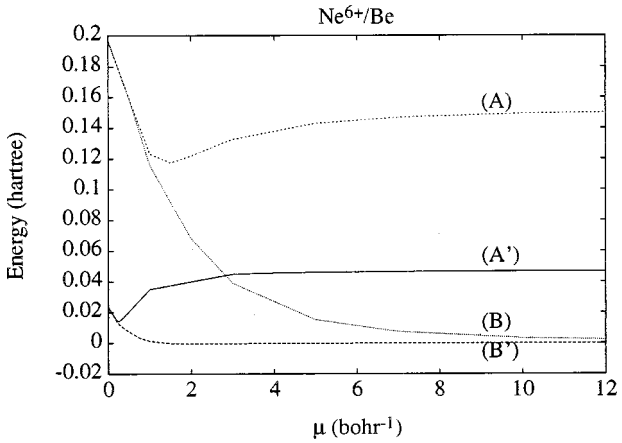

FIG. 6. Variation of the energies of Be and Ne^{6+} with the CI-DF coupling parameter: The (A) curve represents the calculation using the configuration $(2s)^2$ of Ne^{6+}, the (B) curve was obtained by adding the $2p$ natural orbitals to the configuration space of Ne^{6+}, the (A′) curve represents the calculation using the configuration $(2s)^2$ of Be, the (B′) curve was obtained by adding the $2p$ natural orbitals to the configuration space of Be. All the curves have been shifted so that (B) and (B′) energies coincide when $\mu\to\infty$.

TABLE VIII. H_2 at 3 a.u.: Changes of the correlation energy with increasing configuration space. For the explanation of symbols, see Table I. $E_{\mathrm{FCI}} = -1.0570$ a.u., $E_{\mathrm{RHF}} = -0.9893$ a.u., $\langle r_s^{-1}\rangle = 0.45$ bohr^{-1}.

			Percentage of correlation energy		
NO	ON	CSF's	"best" μ	$\langle r_s^{-1}\rangle$	$\mu\to\infty$
$1\sigma_g$	1.794 892 0	1	66.6	60.8	-5.1
$1\sigma_u$	0.195 364 8	2	87.2	72.5	87.0
$2\sigma_g$	0.003 190 9	4	91.1	72.8	91.0
$1\pi_u$	0.002 793 4	6	97.5	73.8	97.5
$3\sigma_g$	0.000 264 3	9	98.0	74.3	98.0
$2\sigma_u$	0.000 135 5	11	98.3	75.1	98.3
$1\pi_g$	0.000 120 7	13	98.8	75.1	98.8

excited configurations to the configuration-space causes the "best" μ to be quite large, implying a very small short-range contribution (see Table IX). Please note that the "best" μ is, however, determined by quite a severe criterion, and that a tolerance of $\sim$1 mhartree would produce much smaller values.

Once again, the system-averaged coupling parameter yields poor results, even with a very large configuration-space.

3. BeH hydride

The BeH hydride is a molecule where strong nondynamical correlation effects take place, as can be seen in Table X, where even with a very large configuration space including up to 178 CSF's, only a moderate accuracy can be reached. Among the necessary NO's, the 1π and 2π NO's cause significant jumps in the percentage of correlation energy.

It should also be noted that the BeH hydride is an open-shell molecule and that our CI-DF coupling method involved a spin-unpolarized short-range exchange-correlation functional.

4. BH hydride

The results reported in Table XI seem to indicate that the BH hydride is an intermediate system where dynamical and nondynamical correlation effects are both important. For such systems, the system-averaged μ seems to be quite reliable, as the correlation energy is greater than with the CI, except for the two largest configuration spaces. Once again, including the 1π and 2π NO's leads to significant improvements.

TABLE IX. H_2 at 3 a.u.: Dependence of the "best" coupling parameter μ on the size of the configuration space. For an explanation of symbols, see Table VII. $E_{\mathrm{FCI}} = -1.0570$ a.u., $E_{\mathrm{RHF}} = -0.9893$ a.u.

NO	"best" μ	$E_{\mathrm{xc,sr}}$
$1\sigma_g$	0.25	-0.286
$1\sigma_u$	5.75	-0.003
$2\sigma_g$	7.50	-0.002
$1\pi_u$	8.50	-0.001
$3\sigma_g$	8.75	-0.001
$2\sigma_u$	9.00	-0.001
$1\pi_g$	9.00	-0.001

TABLE X. BeH: Changes of the correlation energy with increasing configuration space. For the explanation of symbols, see Table I. $E_{\mathrm{MRCI}}=-1.5912$ a.u., $E_{\mathrm{RHF}}=-1.5454$ a.u., $\langle r_s^{-1}\rangle=0.47$ bohr^{-1}.

			Percentage of correlation energy		
NO	ON	CSF's	"best" μ	$\langle r_s^{-1}\rangle$	$\mu\to\infty$
3σ	0.989 967 0	1	62.8	61.9	−1.9
3σ	0.989 967 0	2	62.9	62.0	−1.1
4σ	0.015 624 0	8	65.1	63.8	28.8
1π	0.015 046 0	14	75.2	67.9	52.2
5σ	0.007 875 7	28	78.9	68.8	66.9
2π	0.004 012 4	52	91.3	72.5	86.1
6σ	0.001 345 7	80	93.5	74.0	88.4
7σ	0.000 394 9	118	94.3	74.8	89.7
3π	0.000 329 7	178	96.1	75.4	92.3

TABLE XI. BH: Changes of the correlation energy with increasing configuration space. For the explanation of symbols, see Table I. $E_{\mathrm{MRCI}}=-3.2522$ a.u., $E_{\mathrm{RHF}}=-3.1464$ a.u., $\langle r_s^{-1}\rangle=0.56$ bohr^{-1}.

			Percentage of correlation energy		
NO	ON	CSF's	"best" μ	$\langle r_s^{-1}\rangle$	$\mu\to\infty$
3σ	1.853 418 4	1	71.9	69.6	−0.9
1π	0.065 985 7	8	77.8	77.7	39.3
4σ	0.022 641 5	19	79.3	79.3	51.8
5σ	0.008 203 9	41	80.4	80.4	60.6
2π	0.007 154 3	104	86.0	84.0	77.1
6σ	0.006 492 6	172	89.0	84.7	84.2
7σ	0.001 982 7	273	91.2	85.3	87.7
3π	0.001 004 3	504	93.8	85.6	91.3

TABLE XII. B_2: Changes of the correlation energy with increasing configuration space. For the explanation of symbols, see Table I. $E_{\mathrm{MRCI}}=-5.3382$ a.u., $E_{\mathrm{RHF}}=-5.1230$ a.u., $\langle r_s^{-1}\rangle=0.52$ bohr^{-1}.

			Percentage of correlation energy		
NO	ON	CSF's	"best" μ	$\langle r_s^{-1}\rangle$	$\mu\to\infty$
$1\pi_u$	0.958 812 2	1	65.9	49.8	−3.5
$3\sigma_g$	0.281 461 6	6	68.2	62.3	28.2
$1\pi_g$	0.058 690 4	74	72.5	72.4	52.4
$3\sigma_u$	0.018 036 0	192	74.2	74.2	61.2
$4\sigma_g$	0.008 065 4	432	75.2	75.2	65.6
$1\delta_g$	0.006 664 1	1656	78.9	77.5	72.7
$2\pi_g$	0.005 739 6	4896	83.8	78.9	80.6

TABLE XIII. O_2 at 4 a.u.: Changes of the correlation energy with increasing configuration space. For the explanation of symbols, see Table I. $E_{\mathrm{MRCI}}=-31.7768$ a.u., $E_{\mathrm{RHF}}=-31.0562$ a.u., $\langle r_s^{-1}\rangle=1.01$ bohr^{-1}.

			Percentage of correlation energy		
NO	ON	CSF's	"best" μ	$\langle r_s^{-1}\rangle$	$\mu\to\infty$
$1\pi_g$	1.320 718 9	1	74.7	49.8	−2.5
$1\pi_g$	1.320 718 9	2	79.0	69.8	22.5
$3\sigma_u$	0.556 819 0	48	87.1	84.4	49.5
$2\pi_u$	0.014 723 7	2588	87.7	85.5	52.7
$4\sigma_g$	0.009 357 1	12282	88.2	86.1	55.4
$2\pi_g$	0.007 731 6	161104	88.7	87.4	61.4

5. B_2 dimer

The B_2 dimer could also be seen as an intermediate system where dynamical and nondynmical correlation effects are crucial. However, the results reported in Table XII reveal the importance of the virtual NO's. Even with the largest configuration-space, that includes up to 4896 CSF's, only a moderate accuracy can be achieved.

In order to improve the calculations on the B_2 dimer, spin dependence should probably be taken into account in our short-range exchange-correlation functionals.

6. O_2 dimer at large bond distance

We have previously shown that nondynamical correlation effects in the O_2 dimer at equilibrium distance are weak. Nonetheless, by stretching the bond, it is possible to "switch" to a state where near-degeneracy becomes relevant. Such a situation can be found when $R=4$ bohr.

Table XIII shows that one can link the percentage of correlation energy recovered by the single Slater determinant wave function, which is lower than 75%, to the large occupation number of the $3\sigma_u$ NO. Additional NO's increase only slightly the percentage of correlation energy. The system-averaged coupling parameter, while missing a few percents in comparison to "best" μ, yields much better results than pure CI.

V. CONCLUSION

The influence of the size of the configuration space in a method that combines short-range density functionals with long-range wave functions has been studied for a few atoms and molecules. As far as "normal" systems are concerned, a short-range LDA exchange-correlation functional always yield better energies than the conventional one. Furthermore, a system-averaged coupling parameter based on a simple local approximation is reliable enough to yield rather accurate correlation energies. For "abnormal" systems, a reasonable accuracy can only be achieved by enlarging the configuration space. Its size then depends on the quality of the short-range DF and on the spin-polarization of the system. For such systems, the system-average fails to yield good results. In order to improve the method, approximate exchange-correlation functionals that go beyond LDA should be needed, and spin dependence should be handled, either by conventional spin density functional theory or by the alternative on-top pair-density[29–32] interpretation.

[1] O. Sinanoğlu and K. A. Brueckner, *Three Approaches to Electron Correlation in Atoms* (Yale University Press, New Haven, 1970).
[2] M. A. Buijse and E. J. Baerends, *Density Functional Theory of Molecules, Clusters, and Solids* (Kluwer Academic, The Netherlands, 1995), p. 1.
[3] A. D. Becke, *Modern Electronic Structure Theory* (World Scientific, Singapore, 1995), Vol. 2, p. 1022.
[4] W. Kohn and L. J. Sham, Phys. Rev. A **140**, 1133 (1965).
[5] J. P. Perdew, Phys. Rev. B **33**, 8822 (1986).
[6] A. D. Becke, Phys. Rev. A **38**, 3098 (1988).
[7] C. Lee, W. Yang, and R. G. Parr, Phys. Rev. B **37**, 785 (1988).
[8] J. P. Perdew, J. A. Chevary, S. H. Vosko, K. A. Jackson, M. R. Pederson, D. J. Singh, and C. Fiolhais, Phys. Rev. B **46**, 6671 (1992).
[9] O. V. Gritsenko, P. R. T. Schipper, and E. J. Baerends, J. Chem. Phys. **107**, 5007 (1997).

[10] C. D. Sherrill, M. S. Lee, and M. Head-Gordon, Chem. Phys. Lett. **302**, 425 (1999).
[11] E. K. Gross, L. N. Oliveira, and W. Kohn, Phys. Rev. A **37**, 2809 (1988).
[12] J. C. Slater, J. B. Mann, T. M. Wilson, and J. H. Wood, Phys. Rev. **184**, 672 (1969).
[13] B. I. Dunlap, J. Chem. Phys. **78**, 4997 (1983).
[14] B. I. Dunlap, J. Chem. Phys. **29**, 2902 (1984).
[15] S. G. Wang and W. H. E. Schwarz, J. Chem. Phys. **105**, 4641 (1996).
[16] J. F. Janak, Phys. Rev. B **18**, 7165 (1978).
[17] A. Savin, *Density Functional Methods in Chemistry* (Springer, Berlin, 1991), p. 213.
[18] W. Kohn and W. Hanke (unpublished).
[19] H. Stoll and A. Savin, *Density Functional Methods in Physics* (Plenum, New York, 1985), p. 177.
[20] A. Savin and H.-J. Flad, Int. J. Quantum Chem. **56**, 327 (1995).
[21] W. Kohn, Y. Meir, and D. E. Makarov, Phys. Rev. Lett. **80**, 4153 (1998).
[22] M. Levy, Proc. Natl. Acad. Sci. U.S.A. **76**, 6062 (1979).
[23] S. Kurth and J. P. Perdew, Phys. Rev. B **59**, 10461 (1999).
[24] D. L. Freeman, Phys. Rev. B **15**, 5512 (1977).
[25] S. H. Vosko, L. Wilk, and M. Nusair, Can. J. Phys. **58**, 1200 (1980).
[26] A. Savin, *Recent Developments and Applications of Modern Density Functional Theory* (Elsevier, Amsterdam, 1996), p. 327.
[27] G. D. Mahan, *Many-Particle Physics* (Plenum, New York, 1990).
[28] He, Li, Be, B, C, N, O, F, Li^+, Be^+, B^+, N^+, O^+, F^+, O^-, F^-, LiH, BeH, BH, CH, NH, OH, FH, LiH^+, BeH^+, BH^+, NH^+, OH^+, FH^+, Li_2, Be_2, B_2, C_2, N_2, O_2, F_2, Li_2^+, Be_2^+, B_2^+, C_2^+, N_2^+, O_2^+, F_2^+, Be^{2+}, B^{3+}, C^{4+}, N^{5+}, O^{6+}, Ne^{8+}, C^{2+}, N^{3+}, O^{4+}, F^{5+}, Ne^{6+}.
[29] F. Moscardo and E. San-Fabian, Phys. Rev. A **44**, 1549 (1991).
[30] A. D. Becke, A. Savin, and H. Stoll, Theor. Chim. Acta **91**, 147 (1995).
[31] J. P. Perdew, A. Savin, and K. Burke, Phys. Rev. A **51**, 4531 (1995).
[32] J. P. Perdew, M. Ernzerhof, K. Burke, and A. Savin, Int. J. Quantum Chem. **61**, 197 (1997).
[33] G. C. Lie and E. Clementi, J. Chem. Phys. **60**, 1275 (1974).
[34] G. C. Lie and E. Clementi, J. Chem. Phys. **60**, 1288 (1974).
[35] P. A. M. Dirac, Proc. Cambridge Philos. Soc. **26**, 376 (1930).
[36] P. O. Löwdin, Phys. Rev. **97**, 1474 (1955).
[37] The corresponding active spaces of the reference wave functions, represented by the last NO in each symmetry, are listed here in the case where the number of electrons is larger than two: 4σ, 1π for BeH and for BH, $2s$, $2p$ for Be, $3\sigma_g$, $3\sigma_u$, $1\pi_u$, $1\pi_g$ for B_2, and $3\sigma_g$, $3\sigma_u$, $2\pi_u$, $1\pi_g$ for O_2.
[38] T. H. Dunning, Jr., J. Chem. Phys. **90**, 1007 (1989).
[39] D. E. Woon and T. H. Dunning, Jr., J. Chem. Phys. **100**, 2975 (1994).
[40] A. Bergner, M. Dolg, W. Kuechle, H. Stoll, and H. Preuss, Mol. Phys. **80**, 1431 (1993).
[41] M. E. Mura and P. J. Knowles, J. Chem. Phys. **24**, 9848 (1996).
[42] A. D. Becke, J. Chem. Phys. **88**, 2547 (1988).
[43] MOLPRO is a package of *ab initio* programs written by H.-J. Werner and P. J. Knowles, with contributions from R. D. Amos, A. Berning, D. L. Cooper *et al.*
[44] H.-J. Werner and P. J. Knowles, J. Chem. Phys. **89**, 5803 (1988).
[45] P. J. Knowles and H.-J. Werner, Chem. Phys. Lett. **145**, 514 (1985).
[46] T. Leininger, H. Stoll, H.-J. Werner, and A. Savin, Chem. Phys. Lett. **275**, 151 (1997).
[47] This quantity is not very sensitive to the level of theory.
[48] C. L. Perkeris, Phys. Rev. **115**, 1216 (1959).
[49] W. Kolos and L. Wolniewicz, J. Chem. Phys. **49**, 404 (1968).